Available online at www.sciencedirect.com
SCIENCE DIRECT®
PHYSICS LETTERS B
Physics Letters B 581 (2004) 75–81
www.elsevier.com/locate/physletb

Electromagnetic form factor of the pion in the space- and time-like regions within the front-form dynamics

J.P.B.C. de Melo [a], T. Frederico [b], E. Pace [c], G. Salmè [d]

[a] Instituto de Física Teórica, Universidade Estadual Paulista, 01405-900 São Paulo, SP, Brazil
[b] Departamento de Física, Instituto Tecnológico da Aeronáutica, Centro Técnico Aeroespacial, 12.228-900 São José dos Campos, São Paulo, Brazil
[c] Dipartimento di Fisica, Università di Roma "Tor Vergata" and Istituto Nazionale di Fisica Nucleare, Sezione Tor Vergata, Via della Ricerca Scientifica 1, I-00133 Roma, Italy
[d] Istituto Nazionale di Fisica Nucleare, Sezione Roma I, P.le A. Moro 2, I-00185 Roma, Italy

Received 10 November 2003; accepted 28 November 2003

Editor: P.V. Landshoff

Abstract

The pion electromagnetic form factor is calculated in the space- and time-like regions from -10 $(\mathrm{GeV}/c)^2$ up to 10 $(\mathrm{GeV}/c)^2$, within a front-form model. The dressed photon vertex where a photon decays in a quark–antiquark pair is depicted generalizing the vector meson dominance ansatz, by means of the vector meson vertex functions. An important feature of our model is the description of the on-mass-shell vertex functions in the valence sector, for the pion and the vector mesons, through the front-form wave functions obtained within a realistic quark model. The theoretical results show an excellent agreement with the data in the space-like region, while in the time-like region the description is quite encouraging.

PACS: 12.39.Ki; 12.40.Vv; 13.40.Gp; 14.40.Aq

Keywords: Relativistic quark model; Vector-meson dominance; Electromagnetic form factors; Pion

In the framework of the front-form dynamics [1] (see, e.g., [2,3] for extensive reviews) a large number of papers has been devoted to the study of the electromagnetic form factor of the pion, mostly dealing with the space-like (SL) region [4–10]. To our knowledge, in the front-form quantization the elastic time-like (TL) form factor has only been calculated in a scalar field theory model for $q\bar{Q}$ mesons with point-like vertices [11].

In this Letter, the pion electromagnetic form factor is evaluated within the front-form dynamics, in both the SL and the TL regions, by using as a starting point the Mandelstam formula [12] for the triangle diagrams of Figs. 1 and 2. Our aim is to investigate the possibility of describing the photon–hadron interaction by applying the vector meson (VM) dominance ansatz (see, e.g., [13]) at the level of the photon vertex function.

E-mail address: salmeg@roma1.infn.it (G. Salmè).

0370-2693
doi:10.1016/j.physletb.2003.11.072

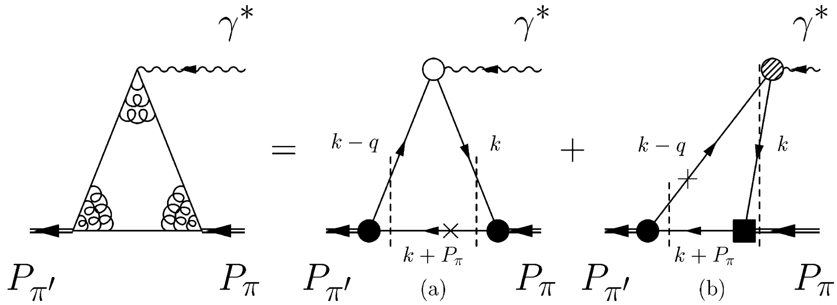

Fig. 1. Diagrammatic representation of the pion elastic form factor for $q^+ > 0$ vs. the global x^+-time flow. Diagram (a) ($0 \leqslant -k^+ \leqslant P_\pi^+$) is the contribution of the valence component in the initial pion wave function. Diagram (b) ($P_\pi^+ \leqslant -k^+ \leqslant P_\pi'^+$) is the non-valence contribution to the pion form factor. Both processes contain the contribution from the dressed photon vertex. The crosses correspond to the quarks on the k^- shell (see text).

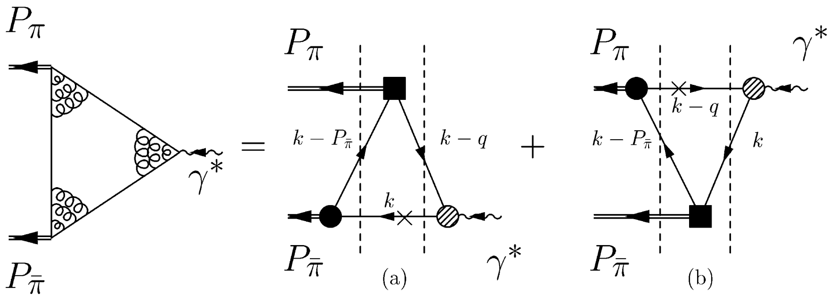

Fig. 2. Diagrammatic representation of the photon decay ($\gamma^* \to \pi\bar\pi$) vs. the global x^+-time flow. Diagrams (a) and (b) correspond to different x^+-time orderings. The crosses correspond to the quarks on the k^- shell (see text).

The virtual processes where a quark absorbs or radiates a pion are present in both the SL and the TL regions (see the square blobs in Figs. 1(b) and 2(a), (b), respectively) [10]. In a recent study of decay processes within the front-form dynamics [14] the amplitude for the pion emission from a quark was described by a pseudoscalar coupling of quark and pion fields, multiplied by a constant. Here, we just follow this suggestion, and use a constant to parametrize the amplitudes for the radiative pion absorption or emission by a quark.

In order to simplify our calculations, we evaluate the pion form factor for a vanishing pion mass, i.e., at the chiral limit. As a consequence, the gap between the SL region and the TL one (i.e., between $q^2 \leqslant 0$ and $q^2 \geqslant 4m_\pi^2$) disappears.

Our starting point is the Mandelstam covariant expression [12] of the amplitudes for the processes $\pi\gamma^* \to \pi'$, or $\gamma^* \to \pi\pi'$, where the meson π' is a pion in the elastic case or an antipion in the production process. For the TL region one has (see Fig. 2)

$$
\begin{aligned}
j^\mu = {} & -\imath e 2 \frac{m^2}{f_\pi^2} N_c \\
& \times \int \frac{d^4k}{(2\pi)^4} \bar\Lambda_{\pi'}(k-P_\pi, P_{\pi'}) \bar\Lambda_\pi(k, P_\pi) \\
& \times \operatorname{Tr}\big[S(k-P_\pi)\gamma^5 S(k-q) \Gamma^\mu(k,q) S(k)\gamma^5\big],
\end{aligned} \tag{1}
$$

where $N_c = 3$ is the number of colors; $S(p) = \frac{1}{\not p - m + \imath\epsilon}$, with m the mass of the constituent quark; q^μ is the virtual photon momentum; $\bar\Lambda_\pi(k, P_\pi)$ the vertex function for the pion, which will be assumed to be a symmetric function of the two quark momenta; P_π^μ and $P_{\pi'}^\mu$ are the pion momenta. The factor 2 stems from isospin algebra. The "bar" notation on the vertex function means that the associated amplitude is the solution of the Bethe–Salpeter equation where the two-body irreducible kernel is placed on the right of the amplitude, while in the conventional case it

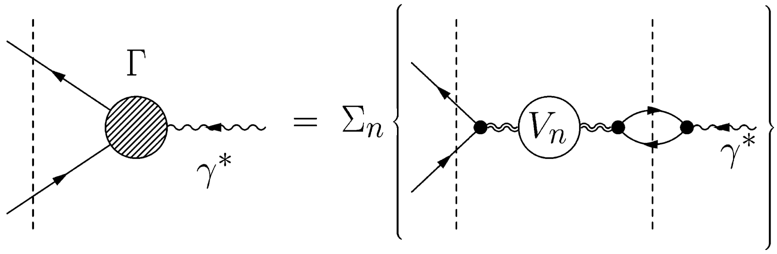

Fig. 3. Dressed photon vertex. The double-wiggly lines represent the front-form Green function describing the vector-meson propagation.

is placed on the left of the Bethe–Salpeter amplitude [15]. For the SL region P_π^μ should be replaced by $-P_\pi^\mu$, and then the initial pion vertex should be written as $\Lambda_\pi(-k, P_\pi) = \bar{\Lambda}_\pi(k, -P_\pi)$.

The central assumption of the Letter is our microscopical description of the dressed photon vertex, $\Gamma^\mu(k,q)$, in the processes where a photon with $q^+ > 0$ decays in a quark–antiquark pair at equal light-front times. In these processes we approximate the plus component of the photon vertex, dressed by the interaction between the $q\bar{q}$ pair, as follows (see Fig. 3)

$$\Gamma^+(k,q) = \sqrt{2}\sum_{n,\lambda}\big[\epsilon_\lambda \cdot \hat{V}_n(k,k-q)\big]\Lambda_n(k,P_n) \times \frac{[\epsilon_\lambda^+]^* f_{Vn}}{[q^2 - M_n^2 + \imath M_n \Gamma_n(q^2)]}, \tag{2}$$

where f_{Vn} is the decay constant of the nth vector meson in a virtual photon (see below), M_n the corresponding mass, P_n the VM total momentum ($P_n^\mu \equiv \{P_n^- = (|\mathbf{q}_\perp|^2 + M_n^2)/q^+, \mathbf{P}_{n\perp} = \mathbf{q}_\perp, P_n^+ = q^+\}$; note that at the production vertex, see Fig. 3, the front-form three-momentum is conserved), and ϵ_λ the VM polarization. The total decay width in the denominator is assumed to be vanishing in the SL region, while it is equal to $\Gamma_n(q^2) = \Gamma_n q^2/M_n^2$ in the TL one [16]. For a detailed discussion of Eq. (2) see Ref. [17]. In Eq. (2) the sum runs over all the possible vector mesons, and the quantity $[\epsilon_\lambda \cdot \hat{V}_n(k,k-q)]\Lambda_n(k,q)$ is the VM vertex function. The momentum component, $\Lambda_n(k,P_n)$, of the VM vertex function, evaluated on the quark mass shell (i.e., for $k^- = k^-_{on} = (|\mathbf{k}_\perp|^2 + m^2)/k^+$), will be related for $0 < k^+ < P_n^+$ to the momentum part of the front-form VM wave function [18], which describes the valence component of the meson state $|n\rangle$,

$$\psi_n\big(k^+, \mathbf{k}_\perp; P_n^+, \mathbf{P}_{n\perp}\big) = \frac{P_n^+}{[M_n^2 - M_0^2(k^+, \mathbf{k}_\perp; P_n^+, \mathbf{P}_{n\perp})]} \times \big[\Lambda_n(k,P_n)\big]_{[k^- = k^-_{on}]}. \tag{3}$$

In Eq. (3), $M_0(k^+, \mathbf{k}_\perp; P^+, \mathbf{P}_\perp)$ is the free mass of a $q\bar{q}$ system with total momentum P, and individual kinematical momenta $(k^+, \mathbf{k}_\perp)$ and $(P^+ - k^+, \mathbf{P}_\perp - \mathbf{k}_\perp)$. Since in our model we consider for the moment only the $^3S_1$ vector mesons, we adopt, for the on-the-mass-shell spinorial part of the VM vertex, the form given in Ref. [18] (that generates the well-known Melosh rotations for $^3S_1$ states)

$$\hat{V}_n^\mu(k,k-q) = \gamma^\mu - \frac{k^\mu_{on} - (q-k)^\mu_{on}}{M_0(k^+, \mathbf{k}_\perp; q^+, \mathbf{q}_\perp) + 2m}. \tag{4}$$

The coupling constant, f_{Vn}, of the nth vector meson is defined by the covariant expression [19] $\epsilon_\lambda^\mu \sqrt{2} f_{Vn} = \langle 0|\bar{q}\gamma^\mu q|\phi_{n,\lambda}\rangle$, with $|\phi_{n,\lambda}\rangle$ the VM state. The coupling constant can be obtained from the front-form VM wave function by evaluating this expression with $\mu = +$ and $\lambda = z$, in the rest frame of the resonance, where $P_n^\mu = (M_n, \vec{0})$, $P_n^+ = M_n$ (see Fig. 3). Assuming that $\Lambda_n(k,P_n)$ does not diverge in the complex plane k^- for $|k^-| \to \infty$, and neglecting the contributions of its singularities in the k^- integration, one obtains

$$f_{Vn} = -\imath \frac{N_c}{4(2\pi)^4} \int dk^- \, dk^+ \, d\mathbf{k}_\perp \times \frac{\mathrm{Tr}[\gamma^+ \mathcal{V}_{nz}(k, k-P_n)]\Lambda_n(k,P_n)}{[k^2 - m^2 + \imath\epsilon][(P_n - k)^2 - m^2 + \imath\epsilon]}$$

$$= -\frac{N_c}{4(2\pi)^3}\int_0^{P_n^+} dk^+\, d\mathbf{k}_\perp \frac{\mathrm{Tr}[\gamma^+ \mathcal{V}_{nz}(k,k-P_n)]}{k^+(P_n^+-k^+)} \times \psi_n\big(k^+,\mathbf{k}_\perp; M_n, \vec{0}_\perp\big), \qquad (5)$$

where $\mathcal{V}_{nz}(k,k-P_n) = (\not{k} - \not{P}_n + m)\hat{V}_{nz}(k,k-P_n)(\not{k}+m)$. Since both the quarks are on shell in the front-form wave function and there is symmetry with respect to the two quark momenta, we do not distinguish between $[\Lambda_n(k,P_n)]_{[k^-=k^-_{on}]}$ and $[\Lambda_n(k,P_n)]_{[k^-=P_n^- -(P_n-k)^-_{on}]}$ in the range $0<k^+<P_n^+$. With our assumptions, one obtains the same expression for f_{Vn}, either if the k^- integration is performed in the upper or in the lower complex k^- semiplane.

For a unified description of TL and SL form factors, it is necessary to choose a reference frame where the plus component of the momentum transfer, q^+, is different from zero (otherwise, $q^2 = q^+q^- - q_\perp^2$ cannot be positive). It is well known that the choice of the reference frame has a fundamental role, as shown in previous works in the SL region [7–9,20] and in the TL one [11]. In Ref. [21] it was shown that, within the front-form Hamiltonian dynamics, a Poincaré covariant and conserved current operator can be obtained from the matrix elements of the free current, evaluated in the Breit reference frame, where the initial and the final total momenta of the system are directed along the spin quantization axis, z. Following Ref. [21], we calculate Eq. (1) in a reference frame where $\mathbf{q}_\perp = 0$ and $q^+ > 0$.

Both in the SL and the TL regions, the integration on k^- in Eq. (1) is performed with the assumption that: (i) $\Lambda_\pi(k,P_\pi)$ does not diverge in the complex plane k^- for $|k^-|\to\infty$, and (ii) the contributions of the possible singularities of $\Lambda_\pi(k,P_\pi)$ can be neglected. Also the contributions of the poles in k^- of the photon vertex function, $\Gamma^+(k,q)$, are supposed to be negligible.

Then, in the SL case, where $P^\mu_{\pi'} = P^\mu_\pi + q^\mu$, the current matrix element j^μ becomes the sum of two contributions, corresponding to the diagrams of Fig. 1(a) and (b), respectively, $j^\mu_{\mathrm{SL}} = j^{(\mathrm{I})\mu}_{\mathrm{SL}} + j^{(\mathrm{II})\mu}_{\mathrm{SL}}$ [9]. The contribution $j^{(\mathrm{I})\mu}_{\mathrm{SL}}$ has the integration on k^+ constrained by $-P_\pi^+ \leqslant k^+ \leqslant 0$, and $j^{(\mathrm{II})\mu}_{\mathrm{SL}}$ has the integration on k^+ in the interval $0<k^+<q^+$. The valence component of the pion contributes to $j^{(\mathrm{I})\mu}_{\mathrm{SL}}$ only, while $j^{(\mathrm{II})\mu}_{\mathrm{SL}}$ is the contribution of the pair-production mechanism from an incoming virtual photon with $q^+>0$ [7–9,20,22,23]. In the SL case we adopt a frame where $\mathbf{P}_{\pi\perp} = \mathbf{P}_{\pi'\perp} = \mathbf{0}$, and we obtain $P_\pi^+ = q^+(-1+\sqrt{1-4m_\pi^2/q^2})/2$. Then, in the limit $m_\pi \to 0$ the longitudinal momenta of the pions are $P_\pi^+ = 0$ and $P_{\pi'}^+ = q^+$. Therefore only the contribution of the pair-production mechanism, $j^{(\mathrm{II})\mu}_{\mathrm{SL}}$, survives (Fig. 1(b)). As shown in Ref. [9], in a frame where $q^+>0$, $j^{(\mathrm{II})\mu}_{\mathrm{SL}}(q^2)$ dominates the form factor at high momentum transfer. Moreover, it turns out that in the model of Ref. [9] the momentum region, where $j^{(\mathrm{II})\mu}_{\mathrm{SL}}(q^2)$ starts to dominate the form factor, tends toward zero if the pion mass is artificially decreased, in agreement with our present discussion.

In the TL case, one has $P^\mu_{\pi'} \equiv P^\mu_{\bar\pi}$, $q^\mu = P^\mu_\pi + P^\mu_{\bar\pi}$. The integration range on k^+ for the matrix element of the current, j^μ, can be decomposed in two intervals, $0<k^+<P_\pi^+$ and $P_\pi^+<k^+<q^+$, and then j^μ_{TL} becomes the sum of two contributions, corresponding to different x^+-time orderings (see diagrams in Fig. 2(a) and (b), respectively). In the final state of the $\pi\bar\pi$ pair we make the purely longitudinal choice, $\mathbf{P}_{\bar\pi\perp} = -\mathbf{P}_{\pi\perp} = \mathbf{0}$. Then, one obtains $P_\pi^+/q^+ = x_\pi = (1\pm\sqrt{1-4m_\pi^2/q^2})2$. In the limit $m_\pi\to 0$, one has $x_\pi = 1$ or 0. Analogously to the SL case, in what follows we adopt the choice $x_\pi = 0$, which implies $P_\pi^+ = 0$ and $P_{\bar\pi}^+ = q^+$. Therefore only the contribution corresponding to the diagram of Fig. 2(b) survives.

The form factor of the pion in the TL and in the SL regions can be obtained from the plus component of the proper current matrix elements: $j^\mu_{\mathrm{TL}} = \langle\pi\bar\pi|\bar q\gamma^\mu q|0\rangle = (P^\mu_\pi - P^\mu_{\bar\pi})F_\pi(q^2)$, and $j^\mu_{\mathrm{SL}} = \langle\pi|\bar q\gamma^\mu q|\pi'\rangle = (P^\mu_\pi + P^\mu_{\pi'})F_\pi(q^2)$ Since in the limit $m_\pi\to 0$ the form factor receives contributions only from the diagrams of Figs. 1(b) and 2(b), where the photon decays in a $q\bar q$ pair, one can apply our approximation for the plus component of the dressed photon vertex (2), both in the SL and in the TL regions. Then the matrix element j^+ can be written as a sum over the vector mesons and consequently the form factor becomes

$$F_\pi\big(q^2\big) = \sum_n \frac{f_{Vn}}{q^2 - M_n^2 + \imath M_n\Gamma_n(q^2)} g^+_{Vn}\big(q^2\big), \qquad (6)$$

where $g^+_{Vn}(q^2)$, for $q^2 > 0$, is the form factor for the VM decay in a pair of pions.

Each VM contribution to the sum (6) is invariant under kinematical front-form boosts and therefore it can be evaluated in the rest frame of the corresponding resonance. In this frame one has $q^+ = M_n$ and $q^- = q^2/M_n$ for the photon and $P^+_n = P^-_n = M_n$ for the vector meson. This means that we choose a different frame for each resonance (always with $\mathbf{q}_\perp = 0$), but all the frames are related by kinematical front-form boosts along the z axis to each other, and to the frame where $q^+ = -q^- = \sqrt{-q^2}$ ($q_z = \sqrt{-q^2}$), adopted in previous analyses of the SL region [9,21]. Since in our reference frame one has $\sum_\lambda [\epsilon^+_\lambda(P_n)]^* \epsilon_\lambda(P_n) \cdot \hat{\Gamma}_n = [\epsilon^+_z(P_n)]^* \epsilon_z(P_n) \cdot \hat{\Gamma}_n = -\hat{\Gamma}_{nz}$, we obtain from Eqs. (1)–(3)

$$
\begin{aligned}
&g^+_{Vn}\big(q^2\big) \\
&\quad = \frac{N_c}{8\pi^3}\frac{\sqrt{2}}{P^+_{\bar\pi}}\frac{m}{f_\pi}\int_0^{q^+}\frac{dk^+}{(k^+)^2(q^+ - k^+)} \\
&\qquad \times \int d\mathbf{k}_\perp \,\mathrm{Tr}\big[\big[\Theta^z \bar{\Lambda}_\pi(k; P_\pi)\big]_{(k^- = q^- + (k-q)^-_{on})}\big] \\
&\qquad \times \psi^*_{\bar\pi}\big(k^+, \mathbf{k}_\perp; P^+_{\bar\pi}, \mathbf{P}_{\bar\pi\perp}\big) \\
&\qquad \times \frac{[M^2_n - M^2_0(k^+, \mathbf{k}_\perp; q^+, \mathbf{q}_\perp)]}{[q^2 - M^2_0(k^+, \mathbf{k}_\perp; q^+, \mathbf{q}_\perp) + i\epsilon]} \\
&\qquad \times \psi_n\big(k^+, \mathbf{k}_\perp; q^+, \mathbf{q}_\perp\big), \qquad (7)
\end{aligned}
$$

where $\Theta^z = \mathcal{V}_{nz}(k, k-q)\gamma^5[\not{k} - \not{P}_\pi + m]\gamma^5$. To obtain Eq. (7) we have first performed the k^- integration, and then we have related $[\bar{\Lambda}_{\bar\pi}(k - P_\pi, P_{\bar\pi})]_{(k^- = q^- + (k-q)^-_{on})}$ in the valence sector to the momentum component of the corresponding front-form pion wave function through the following equation (see Eq. (3))

$$
\begin{aligned}
&\psi_\pi\big(k^+, \mathbf{k}_\perp; P^+_\pi, \mathbf{P}_{\pi\perp}\big) \\
&\quad = \frac{m}{f_\pi}\frac{P^+_\pi [\Lambda_\pi(k, P_\pi)]_{[k^- = k^-_{on}]}}{[m^2_\pi - M^2_0(k^+, \mathbf{k}_\perp; P^+_\pi, \mathbf{P}_{\pi\perp})]}. \qquad (8)
\end{aligned}
$$

As for the VM vertex function, we do not distinguish between $[\Lambda_\pi(k, P_\pi)]_{[k^- = k^-_{on}]}$ and $[\Lambda_\pi(k, P_\pi)]_{[k^- = P^-_\pi - (P_\pi - k)^-_{on}]}$, in the range $0 < k^+ < P^+_\pi$.

Following Ref. [14], in our model the momentum part of the quark-pion emission vertex in the non-valence sector which appears in Eq. (7), $\frac{m}{f_\pi}[\bar{\Lambda}_\pi(k; P_\pi)]_{(k^- = q^- + (k-q)^-_{on})}$ (see the square blob in Fig. 2(b)), is assumed to be a constant. The value of the constant is fixed by the pion charge normalization. The same constant value is assumed for the quark-pion absorption vertex (see the square blob in Fig. 1(b)).

Let us stress that, within our assumptions, $g^+_{Vn}(q^2)$ is given by the same expression both in the TL and in the SL ($P_\pi \to -P_\pi$, see below Eq. (1)) regions. Indeed in the limit $m_\pi \to 0$, one has $P^+_\pi = 0$, $\mathbf{P}_{\pi\perp} = 0$, and $\pm P^-_\pi = q^2/M_n$ with the positive (negative) sign in the TL (SL) region, and therefore the sign in front of $\not{P}_\pi$ in the quantity Θ^z of Eq. (7) has no effect. Then the form factor is continuous in this limit, at $q^2 = 0$. It turns out that for $m_\pi = 0$ only the instantaneous terms (in x^+-time, see, e.g., [9]) contribute to Eq. (7) [17].

In order to describe the pion and the interacting $q\bar{q}$ pairs in the 1^- channel, we use the eigenfunctions of a square mass operator proposed in Refs. [24,25], within a relativistic constituent quark model. This model takes into account confinement through a harmonic oscillator potential and the π–ρ splitting through a Dirac-delta interaction in the pseudoscalar channel. It achieves a satisfactory description of the experimental masses for both singlet and triplet S-wave mesons, with a natural explanation of the "Iachello–Anisovitch law" [26,27], namely the almost-linear relation between the square mass of the excited states and the radial quantum number n. Since the model of Refs. [24,25] does not include the mixing between isoscalar and isovector mesons, in this Letter we include only the contributions of the isovector ρ-like vector mesons.

The eigenfunction $\psi_n(k^+, \mathbf{k}_\perp; q^+, \mathbf{q}_\perp)$, which describes the valence component of the meson state $|n\rangle$, is normalized to the probability of the lowest $(q\bar{q})$ Fock state (i.e., of the valence component). The $q\bar{q}$ probability can be roughly estimated to be $\sim 1/\sqrt{2n + 3/2}$ in a simple model [17] that reproduces the "Iachello–Anisovitch law" [26,27], and is based on an expansion of the VM state $|n\rangle$, in terms of properly weighted Fock states $|i\rangle_0$, with $i > 0$ quark–antiquark pairs.

Our calculation of the pion form factor contains a very small set of parameters: (i) the constituent quark mass, (ii) the oscillator strength, ω, and (iii) the VM widths, Γ_n, for $M_n > 2.150$ GeV. The up-down quark mass is fixed at 0.265 GeV [25]. For the first four vector mesons the known experimental masses and widths are used in the calculations [28]. However, the non-trivial q^2 dependence of $g^+_{Vn}(q^2)$ in our microscopical model implies a shift of the VM masses, with respect to the values obtained by using Breit–Wigner functions with constant values for g^+_{Vn}. As a consequence, the value of the ρ meson mass is moved in our model from the usual one, 0.775 to 0.750 GeV. For the other VM, the mass values corresponding to the model of Ref. [25] are used, while for the unknown widths we use a single value $\Gamma_n = 0.15$ GeV, which presents the best agreement with the compilation of the experimental data of Ref. [29]. We consider 20 resonances in our calculations to obtain stability of the results up to $q^2 = 10\ (\mathrm{GeV}/c)^2$.

The oscillator strength is fixed at $\omega = 1.39\ \mathrm{GeV}^2$ [27]. The values of the coupling constants, f_{Vn}, are evaluated from the model VM wave functions through Eq. (5). The corresponding partial decay width [19] $\Gamma_{e^+e^-} = 8\pi\alpha^2 f^2_{Vn}/(3M^3_n)$, where α is the fine structure constant, can be considered to be in agreement with the experimental data for the ρ meson ($\Gamma^{\mathrm{th}}_{e^+e^-} = 6.37$ keV, $\Gamma^{\mathrm{exp}}_{e^+e^-} = 6.77 \pm 0.32$ keV), and for ρ' and ρ'' ($\Gamma^{\mathrm{th}}_{e^+e^-} = 1.61$ keV and $\Gamma^{\mathrm{th}}_{e^+e^-} = 1.23$ keV, respectively) to be consistent with the experimental lower bounds ($\Gamma^{\mathrm{exp}}_{e^+e^-} > 2.30 \pm 0.5$ keV and $\Gamma^{\mathrm{exp}}_{e^+e^-} > 0.18 \pm 0.1$ keV, respectively) [28].

We perform two sets of calculations. In the first one, we use the asymptotic form of the pion valence wave function, obtained with $\Lambda_\pi(k, P_\pi) = 1$ in Eq. (8); in the second one, we use the eigenstate of the square mass operator of Refs. [24,25]. The pion radius found for the asymptotic wave function is $r^{\mathrm{asymp}}_\pi = 0.65$ fm and for the full model wave function is $r^{\mathrm{model}}_\pi = 0.67$ fm, to be compared with the experimental value $r^{\mathrm{exp}}_\pi = 0.67 \pm 0.02$ fm [30]. The good agreement with the experimental form factor at low momentum transfers is expected, since we have built-in the generalized ρ-meson dominance.

The calculated pion form factor is shown in Fig. 4 in a wide region of square momentum transfers, from $-10\ (\mathrm{GeV}/c)^2$ up to $10\ (\mathrm{GeV}/c)^2$. A general qualitative agreement with the data is seen, independently of the detailed form of the pion wave function. The results obtained with the asymptotic pion wave function and the full model, present some differences only above $3\ (\mathrm{GeV}/c)^2$. The SL form factor is notably well described, except near $-10\ (\mathrm{GeV}/c)^2$. It has to be stressed that the heights of the TL bumps directly depend on the calculated values of f_{Vn} and g^+_{Vn}.

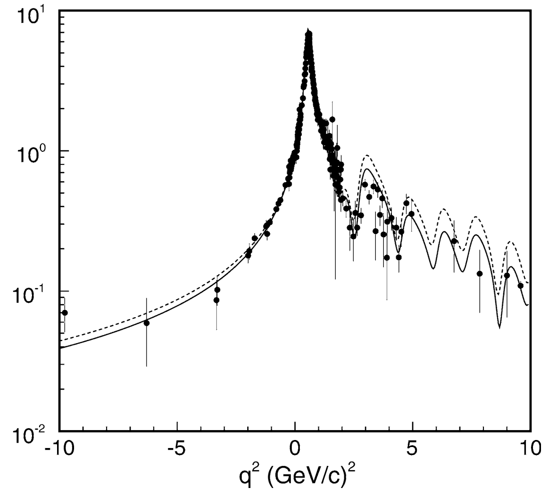

Fig. 4. Pion electromagnetic form factor vs. the square momentum transfer q^2. Dashed and solid lines are the results with the asymptotic (see text) and the full pion wave function, respectively. Experimental data are from Ref. [29].

The introduction of ω-like [31] and ϕ-like mesons could improve the description of the data in the TL region. For instance, the introduction of these mesons could smooth out the oscillations of the form factor at high momentum transfer values. However, a consistent dynamical description of ω-like and ϕ-like states is far beyond the present work, and we leave it for future developments of the model.

Our results show that a VM dominance ansatz for the (dressed photon)-($q\bar{q}$) vertex, within a model consistent with the meson spectrum, is able to give a unified description of the SL and TL pion form factor. Using the experimental widths for the first four vector mesons and a single free parameter for the unknown widths of the other vector mesons, the model gives a qualitative agreement with the TL data, while in the SL region it works surprisingly well. Our VM dominance model can be also applied to evaluate other observables, as the $\gamma^* \to \pi\gamma$ form factor or the nucleon TL form factor.

Acknowledgements

This work was partially supported by the Brazilian agencies CNPq and FAPESP and by Ministero della

Ricerca Scientifica e Tecnologica. J.P.B.C.M. and T.F. acknowledge the hospitality of the Dipartimento di Fisica, Università di Roma “Tor Vergata” and of Istituto Nazionale di Fisica Nucleare, Sezione Tor Vergata and Sezione Roma I.

References

[1] P.A.M. Dirac, Rev. Mod. Phys. 21 (1949) 392.
[2] B.D. Keister, W.N. Polizou, Adv. Nucl. Phys. 20 (1991) 225.
[3] S.J. Brodsky, H.C. Pauli, S.S. Pinsky, Phys. Rep. 301 (1998) 299.
[4] P.L. Chung, F. Coester, W.N. Polizou, Phys. Lett. B 205 (1988) 545.
[5] T. Frederico, G.A. Miller, Phys. Rev. D 45 (1992) 4207;
T. Frederico, G.A. Miller, Phys. Rev. D 50 (1994) 210.
[6] F. Cardarelli, E. Pace, G. Salmè, S. Simula, Phys. Lett. B 357 (1995) 267;
F. Cardarelli, et al., Phys. Rev. D 53 (1996) 6682.
[7] H.W.L. Naus, J.P.C. de Melo, T. Frederico, Few-Body Systems 24 (1998) 99;
J.P.C. de Melo, H.W.L. Naus, T. Frederico, Phys. Rev. C 59 (1999) 2278.
[8] B.L.G. Bakker, H.-M. Choi, C.-R. Ji, Phys. Rev. D 63 (2001) 074014.
[9] J.P.B.C. de Melo, T. Frederico, E. Pace, G. Salmè, Nucl. Phys. A 707 (2002) 399.
[10] C.-W. Hwang, Phys. Rev. D 64 (2001) 034011.
[11] H.-M. Choi, C.-R. Ji, Nucl. Phys. A 679 (2001) 735.
[12] S. Mandelstan, Proc. R. Soc. (London) A 233 (1956) 248.
[13] H.B. O’Connell, et al., Prog. Part. Nucl. Phys. 39 (1997) 201.
[14] C.-R. Ji, H.-M. Choi, Phys. Lett. B 513 (2001) 330.
[15] D. Lurié, A.J. Macfarlane, Y. Takahashi, Phys. Rev. 140 (1965) 1091.
[16] C.J. Gounaris, J.J. Sakurai, Phys. Rev. Lett. 21 (1968) 244.
[17] J.P.B.C. de Melo, T. Frederico, E. Pace, G. Salmè, in preparation.
[18] W. Jaus, Phys. Rev. D 41 (1990) 3394.
[19] W. Jaus, Phys. Rev. D 44 (1991) 2851;
W. Jaus, Phys. Rev. D 60 (1999) 054026;
W. Jaus, Phys. Rev. D 63 (2001) 053009.
[20] J.P.B.C. de Melo, J.H.O. Sales, T. Frederico, P.U. Sauer, Nucl. Phys. A 631 (1998) 574c;
J.P.B.C. de Melo, T. Frederico, H.W.L. Naus, P.U. Sauer, Nucl. Phys. A 660 (1999) 219.
[21] F.M. Lev, E. Pace, G. Salmè, Nucl. Phys. A 641 (1998) 229;
F.M. Lev, E. Pace, G. Salmè, Phys. Rev. Lett. 83 (1999) 5250;
F.M. Lev, E. Pace, G. Salmè, Phys. Rev. C 62 (2000) 064004;
E. Pace, G. Salmè, Nucl. Phys. A 689 (2001) 411.
[22] M. Sawicki, Phys. Rev. D 44 (1991) 433;
M. Sawicki, Phys. Rev. D 46 (1992) 474.
[23] B.L.G. Bakker, H.-M. Choi, C.-R. Ji, Phys. Rev. D 65 (2002) 116001.
[24] T. Frederico, H.-C. Pauli, Phys. Rev. D 64 (2001) 054007.
[25] T. Frederico, H.-C. Pauli, S.-G. Zhou, Phys. Rev. D 66 (2002) 054007;
T. Frederico, H.-C. Pauli, S.-G. Zhou, Phys. Rev. D 66 (2002) 116011.
[26] F. Iachello, N.C. Mukhopadhyay, L. Zhang, Phys. Rev. D 44 (1991) 898.
[27] A.V. Anisovitch, V.V. Anisovich, A.V. Sarantsev, Phys. Rev. D 62 (2000) 051502(R).
[28] K. Hagiwara, et al., Phys. Rev. D 66 (2002) 010001.
[29] R. Baldini, et al., Eur. Phys. J. C 11 (1999) 709;
R. Baldini, et al., Nucl. Phys. A 666–667 (2000) 3;
R. Baldini, et al., private communication.
[30] S.R. Amendolia, et al., Phys. Lett. B 178 (1986) 116.
[31] S. Gardner, H.B. O’Connell, Phys. Rev. D 57 (1998) 2716.